This paper is published as part of a *Dalton Transactions* themed issue entitled:

Application of inorganic chemistry for non-cancer therapeutics

Guest Editor: Katherine J. Franz

Published in issue 21, 2012 of *Dalton Transactions*

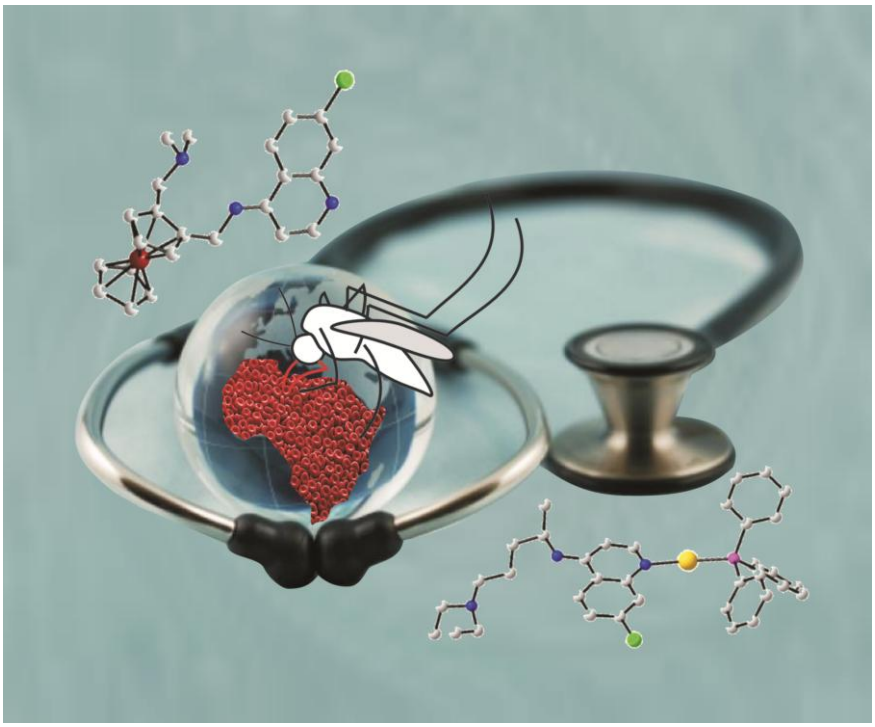

Image reproduced with permission of Christophe Biot

Articles published in this issue include:

Visit the *Dalton Transactions* website for more cutting-edge bioinorganic chemistry research
www.rsc.org/dalton

Dalton Transactions

Dynamic Article Links

Cite this: *Dalton Trans.*, 2012, **41**, 6477

www.rsc.org/dalton

PAPER

Evaluation of the binding of oxovanadium(IV) to human serum albumin†

Isabel Correia,[a] Tamás Jakusch,*[b] Enoch Cobbinna,[a] Sameena Mehtab,[a] Isabel Tomaz,[c] Nóra V. Nagy,[d] Antal Rockenbauer,[d] João Costa Pessoa*[a] and Tamás Kiss*[b,e]

Received 16th November 2011, Accepted 2nd March 2012
DOI: 10.1039/c2dt12193j

The understanding of the biotransformations of insulin mimetic vanadium complexes in human blood and its transport to target cells is an essential issue in the development of more effective drugs. We present the study of the interaction of oxovanadium(IV) with human serum albumin (HSA) by electron paramagnetic resonance (EPR), circular dichroism (CD) and visible absorption spectroscopy. Metal competition studies were done using Cu^{II} and Zn^{II} as metal probes. The results show that $V^{IV}O$ occupies two types of binding sites in albumin, which compete not only with each other, but also with hydrolysis of the metal ion. In one of the sites the resulting $V^{IV}O$–HSA complex has a weak visible CD signal and its X-band EPR spectrum may be easily measured. This was assigned to amino acid side chains of the ATCUN site. The other binding site shows stronger signals in the CD in the visible range, but has a hardly measurable EPR signal; it is assigned to the multi metal binding site (MBS) of HSA. Studies with fatted and defatted albumin show the complexity of the system since conformational changes, induced by the binding of fatty acids, decrease the ability of $V^{IV}O$ to bind albumin. The possibility and importance of ternary complex formation between $V^{IV}O$, HSA and several drug candidates – maltol (mal), picolinic acid (pic), 2-hydroxypyridine-*N*-oxide (hpno) and 1,2-dimethyl-3-hydroxy-4(1*H*)-pyridinone (dhp) was also evaluated. In the presence of maltol the CD and EPR spectra significantly change, indicating the formation of ternary VO–HSA–maltol complexes. Modeling studies with amino acids and peptides were used to propose binding modes. Based on quantitative RT EPR measurements and CD data, it was concluded that in the systems with mal, pic, hpno, and dhp $(V^{IV}OL_2)_n$(HSA) species form, where the maximum value for n is at least 6 (mal, pic). The degree of formation of the ternary species, corresponding to the reaction $V^{IV}OL_2$ + HSA ⇆ $V^{IV}OL_2$(HSA) is hpno > pic ≥ mal > dhp. $(V^{IV}OL)_n$(HSA) type complexes are detected exclusively with pic. Based on the spectroscopic studies we propose that in the $(V^{IV}OL_2)_n$(HSA) species the protein bounds to vanadium through the histidine side chains.

Introduction

The studies carried out to investigate the significance of vanadium as well its compounds in biological systems have led to the discovery of its potential as a therapeutic agent. Many papers have thus reported its insulin-mimetic,[1,2] anti-cancer,[3–6] anti-parasitic,[7,8] anti-microbial[9,10] and anti-spermicidal[11] actions.

Pharmacokinetic and pharmacodynamic evaluations at various stages in drug development are critical for key decision-making. The body has effects on the drug during absorption, distribution, metabolism and elimination (ADME), which may significantly affect its bioavailability. It is considered that most vanadium complexes partly decompose in the acidic pH (~2) of the gastric juice before absorption. Consequently, new species with different membrane permeability properties may be formed and alter the amount and form of the absorbed vanadium.[12] Once in the circulation system there is complex formation with the plasma components: $V^{IV}O$ may interact with both high molecular mass and low molecular mass constituents.[13] Earlier we concluded[12] that the strongest $V^{IV}O$ binder in human serum, apotransferrin (apoTf), is the serum constituent that transports the vanadium to the target cells. However, recent results of studies of the $V^{IV}O$–human serum albumin (HSA) interaction[14] and ternary complex formation between the drug candidate complexes with apoTf[15,16] or HSA[16] inspired us to re-evaluate the possible interactions.

[a]*Centro de Química Estrutural, Instituto Superior Técnico, Av. Rovisco Pais 1, 1049-001 Lisbon, Portugal. E-mail: joao.pessoa@ist.utl.pt; Fax: +351 21846445; Tel: +351 218419268*
[b]*Department of Inorganic and Analytical Chemistry, University of Szeged, Dóm tér 7, Szeged H-6720, Hungary. E-mail: jakusch@chem.u-szeged.hu, tkiss@chem.u-szeged.hu; Fax: +36 625443340; Tel: +36 62544337*
[c]*Centro de Ciências Moleculares e Materiais, Faculdade de Ciências da Universidade de Lisboa, Ed. C8, Campo Grande, Campo Grande, 1749-016 Lisboa, Portugal*
[d]*Institute of Structural Chemistry, Chemical Research Center, Hungarian Academy of Sciences, Pusztaszeri út 59-67, H-1025 Budapest, Hungary*
[e]*Bioinorganic Chemistry Research Group of the Hungarian Academy of Sciences, University of Szeged, P.O. Box 440, Szeged H-6701, Hungary*
†Electronic supplementary information (ESI) available: Additional CD and EPR spectroscopic data. See DOI: 10.1039/c2dt12193j

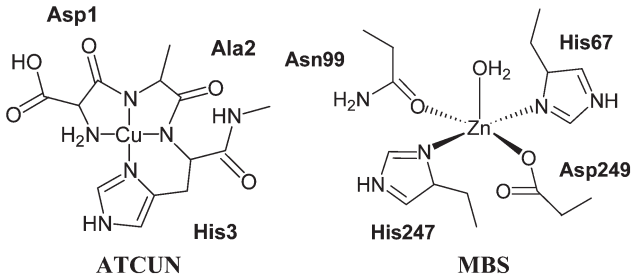

Scheme 1 The ATCUN and MBS binding sites.

Considering its high concentration in plasma it is still believed that albumin may play some role as a transporter of vanadium.[17,18] It should be mentioned here that two recent publications by Sanna *et al.* suggest immunoglobulin G as a weak vanadium(IV) binder in serum, similar to HSA.[19,20]

Albumin has multiple specific and non-specific binding sites where a large number of endogenous and exogenous substances bind. Despite the lack of elaborate structural information about the binding sites of metal ions on albumin, four sites have been described:[21] the ATCUN motif at the N-terminus (N-terminal Cu^{II}- and Ni^{II}-binding site, see Scheme 1) which serves as the primary binding site for Cu^{II} and Ni^{II};[21,22] the multi-metal binding site (MBS, Scheme 1) which primarily binds Zn^{II} and other 2+ metal ions;[23] site B which is the primary binding site for Cd^{II} but can also bind Zn^{II} [21,24] and the reduced thiol of Cys-34, which binds gold and platinum compounds.[21]

The ATCUN motif is one of the best-characterized metal binding sites and it is a suitable site for metal ions which have preference for tetragonal or square-planar coordination. The ATCUN motif has the following sequence in HSA: Asp-1, Ala-2, His-3 and thus, the site provides four nitrogen donors that include the N-terminal amino group, two deprotonated amide nitrogens and the imidazole nitrogen from His-3.

The multi-metal binding site is the principal site for Zn^{II} and the secondary site for Ni^{II} and Cu^{II}, and other 2+ metal ions may bind to this site. The MBS is located at the interface between domains I and II of HSA. Each domain contributes two donors: domain I – His-67 and Asn-99; and domain II – His-247 and Asp-249. The imidazole nitrogens are located in the axial positions of the distorted trigonal bipyramidal arrangement around Zn^{II}. Together with a fifth exogenous ligand, these groups form a distorted trigonal bipyramidal or square-pyramidal site. For Zn^{II}, water is reported to be the 5th ligand.[24,25] Within the neighbourhood of MBS is the location of site II of fatty acids. This site (FA2) is located at the interface between subdomains IA and IIA. The binding of long chain fatty acids (LCFA) at this site causes a rotation of domain I with respect to domain II, resulting in a further separation of His-247 and Asp-249 from His-67 and Asn-99 by 4–6 Å.[21,23,24] As a consequence the MBS site is probably disrupted by the binding of LCFA to the FA2 site, *i.e.* the binding of LCFAs to FA2 and Zn^{II} binding to the MBS site might be mutually exclusive.[25]

Several studies have reported the binding of $V^{IV}O^{2+}$ to albumin.[14,26,27] Two types of binding sites on human and bovine serum albumins have been identified for $V^{IV}O$, being designated by strong and weak sites.[1,28] The strong binding site of $V^{IV}O$ was considered to be the ATCUN motif, which was reported to bind 1 mol equivalent of $V^{IV}O$.[28] The weak binding sites were considered to consist of a number of non-specific interactions that could involve carboxylate or imidazole side chains of amino acid side chains on the albumin.[14,28] By assuming the formation of mononuclear $V^{IV}O$–HSA species, the conditional binding constant of $V^{IV}O$ with HSA has been estimated as $\log K = 9.1 \pm 1.0$,[14] with rather high uncertainty.

Notwithstanding, $V^{IV}O$ binding to amino acid side chains of the ATCUN motif, if occurring, differs from Cu^{II} binding to the same site. $V^{IV}O$ probably does not bind through the amino group of the N-terminal part of the albumin.[1,14,28] Moreover, in studies with small oligopeptides, in the absence of a primary anchor donor group $V^{IV}O$ ions (similarly to Cu^{II}) are not able to induce the deprotonation of the amide groups.[29] The N-terminal amino group is a suitable anchor for Cu^{II}, but not for $V^{IV}O$. So, to date, the actual groups that form the vanadium binding sites are not well known.

The first EPR spectral parameters on HSA at pH 7.4 were reported only in 2005 by Orvig *et al.*[1] Latter, Garribba *et al.* detected a dinuclear $(VO)_2$HSA species by EPR at −150 °C.[14] The spin state of this species is 1, it is observed up to a $V^{IV}O$: HSA ratio of 1 : 1 and the intensity of the spectrum is very low. At $V^{IV}O$: HSA > 1 another type of EPR spectrum (spin 1/2) becomes predominant and no other distinct type of spectrum is observed up to a $V^{IV}O$: HSA ratio of 8 : 1.

Judging from the well-known potential of $V^{IV}O$ and its complexes in the treatment of type-2 diabetes, and its prospective uses for other diseases, it is important to understand its biotransformation, especially how it interacts with transferrin (Tf) and HSA. Extensive work has been done in this regard using various techniques to increase our understanding of the behaviour of $V^{IV}O$ and its complexes in blood.[1,12,14–16,30,31] We have now chosen to study the interaction of $V^{IV}O$ and its complexes with HSA to better characterize the possible species that may form in blood, the nature of the interaction of $V^{IV}O$ with albumin and its binding mode(s) on HSA. By combining EPR and circular dichroism (CD) spectroscopies, and using competition studies involving Cu^{II} and Zn^{II} as metal probes we provide a more holistic approach to obtain information about the composition of the species formed and the $V^{IV}O$ binding sites to HSA. Moreover, to get quantitative information on the HSA–$V^{IV}O$ and HSA–$V^{IV}O$–drug candidate ligand systems quantitative room temperature (RT) EPR measurements were also carried out and evaluated.

Experimental

Materials

Millipore water was used for the preparation of the solutions and HEPES-S buffer was used in all experiments (except RT EPR). This buffer system was adjusted to pH 7.4 using conc. KOH and conc. HCl. The composition of the HEPES-S buffer used was: 50 mM HEPES (Sigma-Aldrich, 99.5%), 25 mM carbonate added as $NaHCO_3$ (Sigma-Aldrich, 99.5%), 1 mM phosphate added as $NaH_2PO_4 \cdot H_2O$ (Merck, 99.0–102%), and 0.20 mM KCl (Merck, 99.5%). For the quantitative RT-EPR measurements another HEPES buffer, also pH 7.4, was used with the following composition: 100 mM HEPES, 85 mM NaCl, 25 mM $NaHCO_3$ and approx. 50 mM NaOH.

The chemical reagents, amino acids and albumins used in this work were used as received from the supplier without further purification. Maltol, picolinic acid, hpno, dhp and $V^{IV}O$-$SO_4 \cdot 4H_2O$ were purchased form Sigma-Aldrich, $CuCl_2 \cdot 2H_2O$ from Merck and $ZnCl_2$ from Riedel-de Häen. The amino acids used in this work include: L-histidine (Merck), glycine-histidine hydrochloride (Sigma-Aldrich), *N*-α-acetyl-L-histidine (Sigma-Aldrich), L-cysteine hydrochloride (BDH), L-histidinol dihydrochloride (Sigma-Aldrich), L-aspartic acid (Sigma-Aldrich) and *S*-ethyl-L-cysteine (Sigma-Aldrich).

Fatted HSA (A1653; 96–99%), crystallized and lyophilized with a molecular mass of 66–67 kDa and defatted HSA (A3782) were purchased from Sigma-Aldrich.

The molecular weight as well as the molar extinction coefficients used for the calculation of albumin concentrations were as follows: fatted HSA and defatted HSA (66.5 kDa; ε(278 nm) = 36 850 M^{-1} cm^{-1})[15,32–34] These values were calculated from information obtained from the indicated references and product information documents from Sigma.

Albumin solutions. The albumin solutions were prepared by dissolving the protein in HEPES-S buffer. The solutions were allowed to stand for at least 30 min to allow them to equilibrate. During this period, they were gently swirled without strong agitation. The concentrations were determined by UV spectrophotometry. Argon was bubbled through all solutions prior to use to displace any oxygen that may be present, and the solutions were kept and manipulated under an argon atmosphere inside a glove bag.

Metal ion solutions. With the exception of the $V^{IV}O$ stock solution {$V^{IV}O(ClO_4)_2$}, which was prepared in 0.010 M HCl, degassed and stored under a nitrogen atmosphere in closed glassware, all other metal ion solutions were freshly prepared by dissolving in Millipore water. The concentration of the stock solutions was as follows: $V^{IV}O(ClO_4)_2$, 9.9 mM; $ZnCl_2$, 54 mM; and $Cu^{II}Cl_2$, 11.7 mM.

Ligand solutions. The amino acid and peptide solutions were prepared by dissolving them in the HEPES-S buffer. The concentrations were in the mM range. When HSA was titrated with complexes (*e.g.* $V^{IV}O(mal)_2$ or $V^{IV}O(pic)_2$) these were prepared *in situ* by mixing the solution of $V^{IV}O(ClO_4)_2$ and the ligands in the chosen ratios. Under these conditions (pH = 7.4 vanadium concentration *ca.* 5–10 mM), some of the complexes were partly (pic: ~85%; mal: <10%; based on speciations) converted to hydrolytic species such as VOA_2OH or $(VOAOH)_2$. Oxidation of vanadium(IV) in these solutions was not observed, due to the careful oxygen free handling.

Titrations. In all titrations the albumin solution (*ca.* 660 μM or *ca.* 1000 μM) was titrated by adding μL aliquots of the other compounds to obtain the desired molar ratios. The CD spectra of the solutions were measured, and samples were taken and frozen at 77 K for LN-EPR measurements.

Spectroscopic measurements

The visible absorption spectra of the solutions were recorded on a Perkin Elmer Lambda 35 UV/Vis spectrophotometer in the range 400–1000 nm. The recordings were done with 1 cm quartz Suprasil® cuvettes. The circular dichroism spectra of the solutions were recorded on a JASCO J-720 spectropolarimeter (JASCO, Hiroshima, Japan) with a red-sensitive photomultiplier (EXEL-308) in the visible region of the electromagnetic spectrum (400–1000 nm). Most of the recordings were done at ~25 °C with a 50 mm quartz cell. The spectra were acquired at a scanning speed of 200 nm min^{-1}; band width of 2.0 nm; response of 2.0 s; sensitivity of 100 mdegree and data pitch of 2 nm. One to three accumulations were made for each measurement.

The X-band EPR (~9.46 GHz) spectra were measured either at room temperature (RT) or at liquid nitrogen (LN) temperature (77 K). The spectra at 77 K were recorded on a Bruker ESP 300E spectrometer. At this temperature the spectra provide adequate information on the symmetry and coordination geometry of the $V^{IV}O$ complexes. The frozen solution also prevents $V^{IV}O$ oxidation. The spectrometer was operated at ~9.46 GHz with a frequency modulation of 100 kHz. While keeping the resolution at either 2048 or 4086 points, the microwave power was adjusted to 20 dB attenuations and the receiver gain was set to either 2.52×10^4 or 6.32×10^4. In order to improve the signal to noise ratio, 10 scans were accumulated for each sample. The spectra acquisition parameters were constant for each batch of experiments. All measurements were done using 3 mm quartz tubes (Wilmad 707-SQ-250M). The EPR samples contained 5% DMSO.

The quantitative RT-EPR spectra were recorded at 298 K using an X-band Bruker EleXsys E500 instrument. Before the measurements, the signal of the capillary tube filled with distilled water was recorded as background.

Calculations

The EPR spectra were simulated with the EPR computer program of Rockenbauer and Korecz.[35] The concentrations of the sum of the species having isotropic or anisotropic spectra (binding or not binding to HSA) were determined by double integration of the spectra. The system was calibrated based on the spectra of simple $V^{IV}O(L)_2$ solutions of known concentration. These concentrations and spectra were used in the input files for determination of stability constants using the computer program PSEQUAD.[36,37] The formed species and the stability constants for the different VO–L systems were taken from the following references: mal,[38] hpno,[13] dhp,[39] and pic.[40]

Results and discussion

The binding sites of HSA

Our room temperature EPR measurements depicted in Fig. 1 show anisotropic spectra due to the interaction of $V^{IV}O$ with HSA, and the slow tumbling of the protein. Most of the paramagnetic vanadium centres are however non-detectable even at a $V^{IV}O$: HSA ratio of 4 : 1. Upon the addition of an excess of dhp to the system (*e.g.* Fig. 1B), the non-EPR-detectable vanadium bound to HSA is sequestered by dhp and the recorded isotropic spectrum of $V^{IV}O(dhp)_2$ appears with much higher intensity. Double integration of such spectra reveals that >90% of the metal ions are in EPR-silent forms. The frozen solution EPR

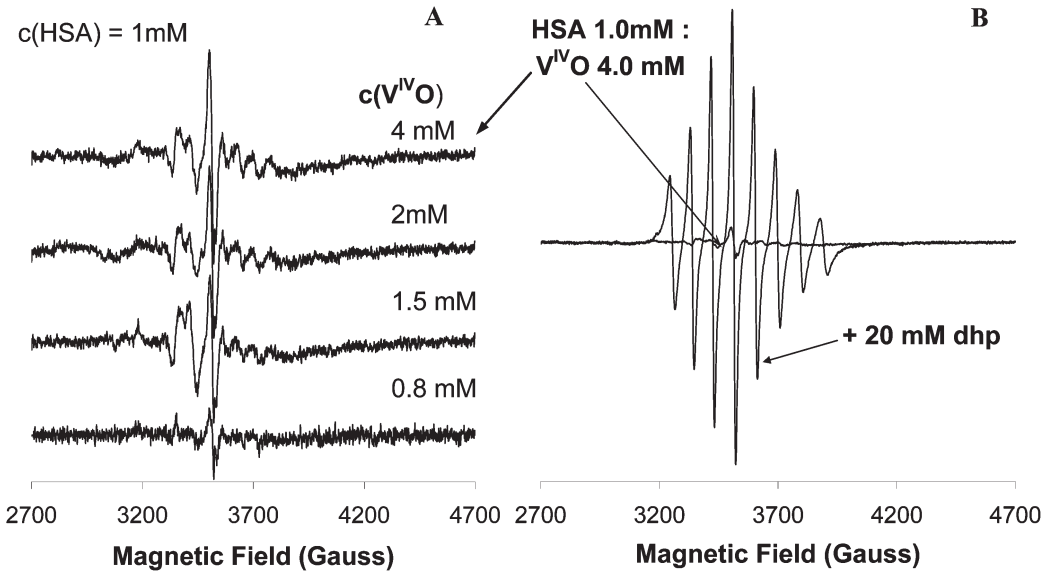

Fig. 1 X-band RT EPR spectra recorded at pH 7.4. (A) 1.0 mM HSA and various amounts of added $V^{IV}O$ stock solution (indicated); (B) superposition of RT EPR spectra of the two following solutions: 1.0 mM HSA + 4.0 mM $V^{IV}O$, and 1.0 mM HSA, 4.0 mM $V^{IV}O$ + 20 mM dhp.

Table 1 EPR parameters of the species formed in the M^{II}-human serum albumin system[35]

			EPR				
M	M : HSA	pH, T (K)	$g_\perp$	$A_\perp$ ($\times 10^4$ cm^{-1})	$g_\parallel$	$A_\parallel$ ($\times 10^4$ cm^{-1})	Ref.
$V^{IV}O$	1 : 1[a]	7.4	1.9628/1.9600[c]	61.70/55.48[c]	1.9265	166.5	1
$V^{IV}O$	≥2 : 1[b]	7.4	1.9628/1.9600[c]	61.70/55.48[c]	1.9355	164.5	1
$V^{IV}O$	≥1 : 1	~5, 120	—	—	1.946	171.2	14
$V^{IV}O$	≥1 : 1	7.4, 120	—	—	1.947	164.6	14
$V^{IV}O$	≤1 : 1	7.4, 120	—	—	1.981	80[d]	14
$V^{IV}O$	≥1 : 1[e]	7.4, RT	1.976(1)[f]	56.1(5)[f]	1.945(1)[f]	164.6(9)[f]	This work
$V^{IV}O$	≥1 : 1	7.4, 77	1.974	58.3	1.941	167.9	This work
Cu^{II}	1 : 1	7.3, 100	2.051	16.0	2.162	208.5	41
Cu^{II}	1 : 1	7.4, 77	2.040	17	2.178	206.3	This work
Cu^{II}	≥1 : 1	7.4, 77	2.053	<5	2.292	162.6	This work

[a] The "strong" site. [b] The "weak" site. [c] Rhombic spectra: g_x/g_y or A_x/A_y. The simulated parameters were fixed for the VO-HSA strong and weak. [d] D value for the dinuclear $(VO)_2$HSA species is 631×10^{-4} cm^{-1}. [e] Room temperature. [f] The error of the last digit in parenthesis.

spectra (77 K) of the same samples were also measured, but we were not able to well reproduce the characteristic weak spectrum of the dinuclear $(VO)_2$HSA species, detected at somewhat higher temperature (−150 °C, ~123 K) by Garribba *et al.*,[14] which was measured by a type of signal averaging which involved repeatedly acquiring the spectrum and adding each one together using a considerable number of spectra.

All the measured spectra can be simulated[35] with one EPR parameter set (Table 1) and the $A_\parallel$ value is in very good agreement with data published earlier.[1,14] An increase in the intensity of the measured spectra was detected as more and more $V^{IV}O$ was added to HSA, however double integration clearly indicated that the growth was not linear. When the $V^{IV}O$ concentration was increased four-fold, only approximately twice as many paramagnetic $V^{IV}O$ centres were detected. Similarly as in the RT EPR experiments, addition of a 20-fold excess of dhp to the samples enhanced the intensity of the spectra considerably (Fig. 1).

These observations suggest that HSA is not able to bind more than one equivalent of EPR-active $V^{IV}O$ ion at pH 7.4. The paramagnetic complex detected is indeed a minor species which is in equilibrium with (most probably) more than one EPR-silent adduct: one of these could be $(V^{IV}O)_2$HSA reported by Garribba *et al.*,[14] and the others probably simply the product of the hydrolysis of $V^{IV}O$ (*e.g.* $[(V^{IV}O)_2(OH)_5]^-$). This might also help to explain why Willsky *et al.*,[42] warned that the complexes formed in the HSA–$V^{IV}O$ system are sensitive to specific solution conditions and aerobic oxidation.

The titration of HSA with $V^{IV}O$ at pH 7.4 yielded the circular dichroism spectra shown in Fig. 2. We must emphasize that each recorded CD spectrum is the sum of the individual contributions of all V^{IV}-centres coordinated at different chiral binding sites with (possibly) different binding donors.

In Fig. 2 it can be seen that when 1 mol equivalent of $V^{IV}O$ is added to defatted HSA, the intensity of the CD spectra is quite weak and the spectrum has a certain pattern (two positive bands

at *ca.* 585 and 710 nm, and one negative at *ca.* 845 nm). When >1 mol equivalent were progressively added the CD intensities of all bands increased significantly with increasing $V^{IV}O$ concentration. However, the pattern of these new CD spectra (one positive band at 590 nm, a shoulder at *ca.* 670 nm, and a negative band at 830 nm) differs from the previous one, but remains the same upon adding $V^{IV}O$ solution up to at least 8 mol equivalents. This appears to reflect the types of binding sites proposed by Orvig, Garribba and Willsky.[1,14,28,42] Up to 1 mol equivalent of $V^{IV}O$ may correspond to one type of binding on HSA (with weak CD signal). Then >1 mol equivalents of $V^{IV}O$ corresponds to the second type of binding. The presence of an isodichroic point at *ca.* 720 nm further suggests the detection of only two chiral $V^{IV}O$–HSA types of binding.

Under normal physiological conditions, HSA carries one or two molecules of LCFA, but up to eight binding sites have been identified.[43] When fatted HSA was used (ESI1†) the intensity of the CD spectra was much lower ($\Delta\varepsilon$ = 0.34 M^{-1} cm^{-1} for defatted *vs.* $\Delta\varepsilon$ = 0.10 M^{-1} cm^{-1} for fatted HSA at 600 nm), confirming that the presence of FA, which may bind at the interface of domains I and II near the MBS, can alter the conformation of HSA to an extent that may disrupt this metal binding site. This also indicates that the site responsible for the observed CD bands is the MBS. Thus, to have a stronger CD signal in the qualitative experiments to probe the HSA binding sites we opted to use defatted HSA, and fatted HSA when carrying out measurements to quantitatively evaluate the binding.

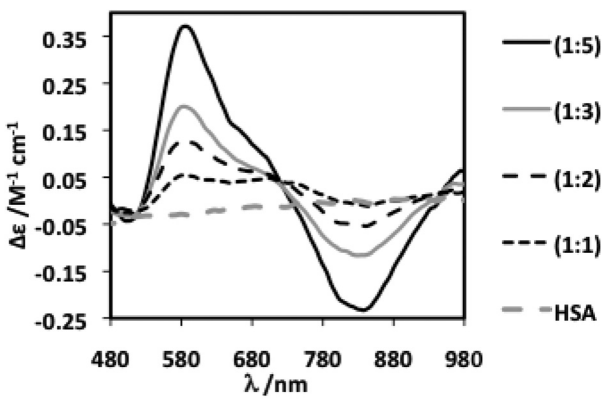

Fig. 2 Circular dichroism spectra of solutions of defatted HSA (0.70 mM) and increasing amounts of $V^{IV}O$ indicated in the figure.

To obtain information on the binding of $V^{IV}O$ to albumin, Zn^{II} was used as a metal probe in metal competition studies. Since Zn^{II} has its d-orbitals fully filled, the species formed when it binds to any of the sites on albumin are not detectable in the X-band EPR and CD spectra. It is known that zinc binds specifically to the MBS, and more strongly than other bivalent metal ions such as Cd^{II}, Ni^{II} and Cu^{II}.[23,24,44] Zinc, apart from the MBS, may also bind to the Cd^{II} main site, also called site B.[24]

The addition of Zn^{II} to a solution containing $V^{IV}O$: HSA at 5 : 1 ratio (c(HSA) = 0.70 mM) up to a total of 1 mol equivalent caused ~65% decrease in the intensity of the positive band at ~590 nm and ~80% in the negative band at ~840 nm (Fig. 3). Further incremental additions of Zn^{II} did not seem to affect much the intensities of the CD bands and the final spectrum resembles that of the 1 : 1 $V^{IV}O$: HSA CD spectrum. This indicates that Zn^{II} substitutes vanadium in the site(s) where we have the most intense CD bands (at ~580 nm and ~830 nm), but not the other sites occupied by $V^{IV}O$. The displacement of $V^{IV}O$ by Zn^{II} is thus only possible at site(s) where Zn^{II} binds strongly: the MBS. Upon the addition of Zn^{II} part of the bound $V^{IV}O^{2+}$ is therefore displaced, it goes to the bulk solution (at pH 7.4) and is extensively hydrolysed. This is the reason why the CD signal becomes much noisier: the intensity of the radiation that reaches the CD detector decreases significantly.

The anisotropic EPR spectral series for the solution containing $V^{IV}O$: HSA at 5 : 1 ratio (ESI2†) showed that a significant part of the $V^{IV}O$ remained bound to HSA when Zn^{II} was added, indicating that there are other sites occupied by $V^{IV}O$. The EPR signals were still observable after addition of 3 mol equivalents of Zn^{II}, and there was no clear change in the EPR spectra except a small reduction in intensity. This suggests that the displaced $V^{IV}O$ was in an EPR-silent form. Near Asp-249, which is one of the donor groups at the MBS, there is one glutamate, which might be used in the coordination to vanadium in a dinuclear form: Glu-252 is at ~5 Å distance from Asp-249. The hyperfine

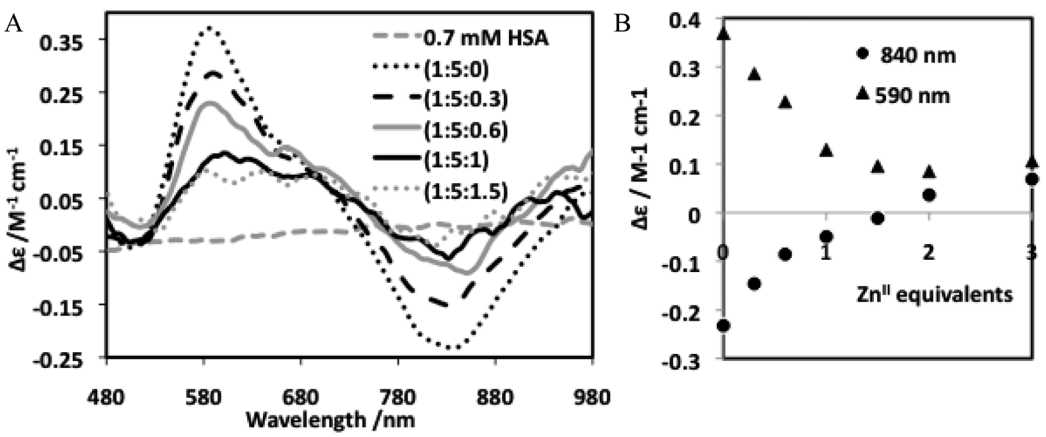

Fig. 3 (A) Circular dichroism spectra of defatted HSA (0.70 mM), $V^{IV}O$: HSA = 5 : 1 and increasing amounts of Zn^{II} (molar ratio indicated in the figure). (B) Variation of $\Delta\varepsilon$ at selected wavelengths with the number of equivalents of Zn^{II} added.

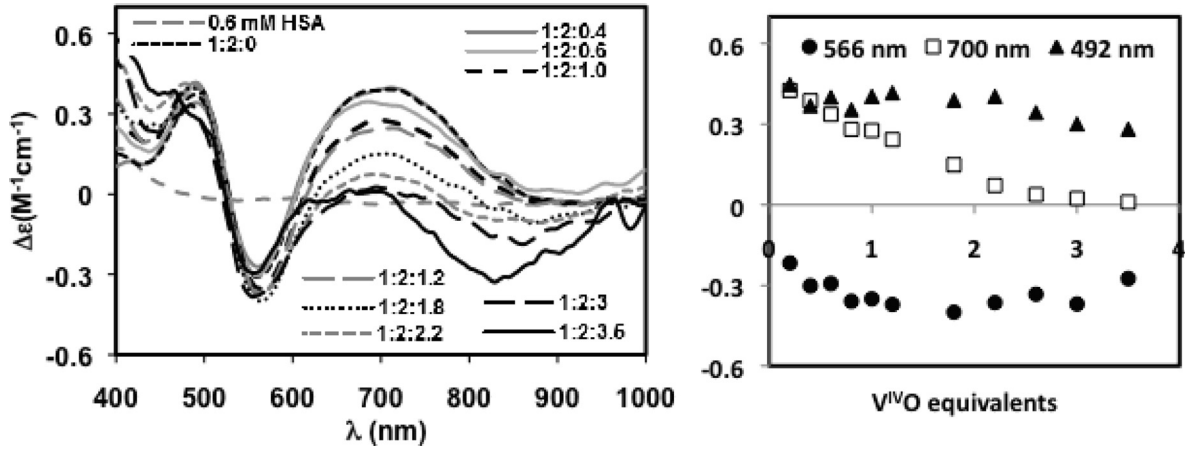

Fig. 4 (A) Circular dichroism spectra of solutions of defatted HSA (0.60 mM), Cu^{II} : HSA = 2 : 1 and upon stepwise additions of $V^{IV}O^{2+}$ (molar ratio indicated in the figure). (B) Variation of $\Delta\varepsilon$ values at selected wavenumbers with the number of equivalents of $V^{IV}O$ added.

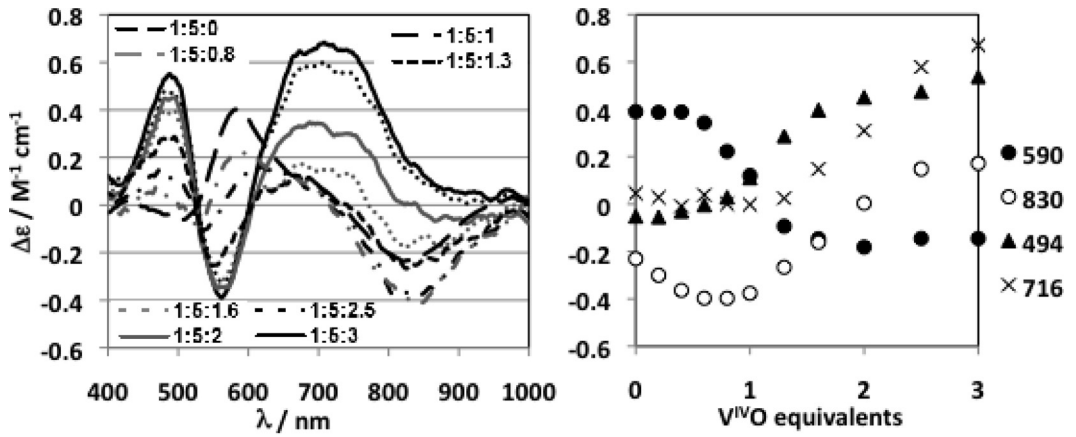

Fig. 5 (A) Circular dichroism spectra of solutions containing defatted HSA (0.50 mM), $V^{IV}O$: HSA = 5 :1 and increasing amounts of Cu^{II} (molar ratios indicated in the figure). (B) Variation of $\Delta\varepsilon$ at selected wavenumbers with the number of equivalents of Cu^{II} added.

coupling parameters of the detected $V^{IV}O$ species were obtained by simulation of the $V^{IV}O$ EPR spectra:[35] $A_{\|} = 167.9 \times 10^{-4}$ cm^{-1} and $g_{\|} = 1.941$, and these agree with the values reported by Orvig[1] and Garribba.[14]

In conclusion, the Zn competition spectroscopic studies indicate that $V^{IV}O$ exhibits two types of binding, one of them corresponding to the MBS. Zn^{II} displaces $V^{IV}O$ from this site, but not from the other sites.

To evaluate the binding of vanadium to side chains at the N-terminus ATCUN site Cu^{II} competition studies were done by CD and EPR spectroscopy. Fig. 4 shows the CD spectra of solutions containing HSA : Cu^{II} : $V^{IV}O$ at 1 : 2 : *x* ratios and pH = 7.4. The CD spectrum of HSA : Cu^{II} with a ratio of 1 : 2 shows a positive band at ~490 nm, a negative one at ~565 nm and a broad positive band centred at ~700 nm. According to several authors[23,45] the bands at 490 and 565 nm are due to the strong coordination of Cu^{II} at the ATCUN site, and the 3rd one to Cu^{II} bound at the MBS.

Our experiments confirmed these assignments and the individual visible CD spectra for Cu^{II} bound at both sites, calculated from the CD spectra, are included in ESI3†. Upon addition of increasing amounts of $V^{IV}O$ to the solution of $(Cu^{II})_2$HSA the broad CD band centred at 700 nm decreased in intensity (see Fig. ESI3-1†) and a new negative one formed at ~820 nm. The EPR data (Fig. ESI3-3†) show that even after the addition of twice the amount of vanadium (*i.e.* ratio 1 : 2 : 4), copper is still bound to HSA in one of the sites. The initial spectrum (ratio 1 : 2 : 1) still shows the presence of two Cu^{II} species with different donor sets, one of them disappearing at the 1 : 2 : 2.2 ratio, when the resonances assignable to a $V^{IV}O$ species are finally observable. This indicates that $V^{IV}O$ is replacing Cu^{II} at the MBS, but not at the ATCUN site.

The EPR spectra of solutions containing HSA, Cu^{II} and $V^{IV}O$ were simulated (ESI3†) and used to calculate the amount of each nuclei at each molar ratio, however, due to the presence of EPR silent species, the exact concentrations can not be calculated. All spectra were simulated and the spin Hamiltonian parameters are included in Table 1.

The reverse experiments were also done: *e.g.* a solution containing HSA was loaded with 5 mol equivalents of $V^{IV}O$ and titrated with Cu^{II}, up to a HSA : $V^{IV}O$: Cu^{II} molar ratio of 1 : 5 : 3. Fig. 5 and 6 show the spectroscopic changes in the CD

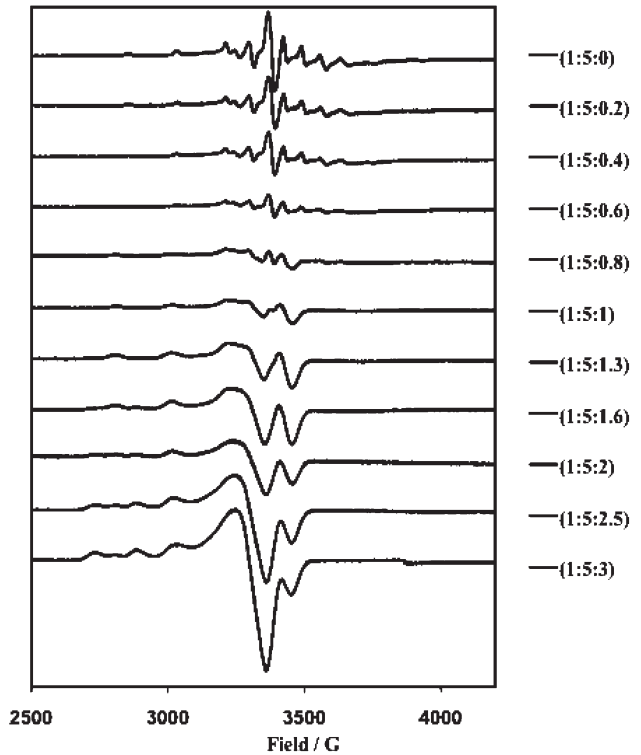

Fig. 6 X-band EPR spectra of solutions containing defatted HSA (0.50 mM), $V^{IV}O$: HSA = 5 : 1 and increasing amounts of Cu^{II} (molar ratios indicated in the figure).

Table 2 The conditional stability constants of the $V^{IV}O$–HSA complexes at pH = 7.4

Complex	Log $\beta \pm 3SD$	Method	Ref.
$(V^{IV}O)_2HSA$	20.9 ± 1.0	EPR (123K)	14
$(V^{IV}O)_2HSA$	20.6 ± 0.4	RT EPR	This work
$(V^{IV}O)HSA$	9.1 ± 1.0	EPR (123K)	14
$(V^{IV}O)HSA$	9.1 ± 0.4	RT EPR	This work

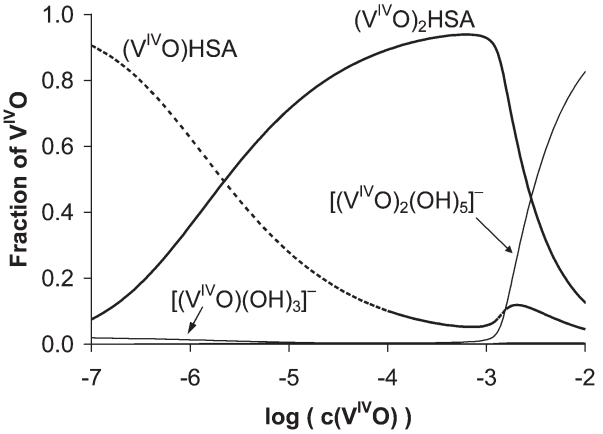

Fig. 7 Speciation curves of the complexes formed in the $V^{IV}O$–HSA system at pH 7.4 and 25.0 °C. c(HSA) = 0.63 mM. The formation constants for $V^{IV}(OH)_3^-$ and $[(V^{IV}O)_2(OH)_5]^-$ were taken from literature.[46,47]

and EPR spectra, respectively. In the CD titration the $V^{IV}O$ negative band at ~830 nm increases its intensity when Cu^{II} is initially added (up to ~0.6 mol equivalents) and then stabilizes, while the Cu^{II} band at ~495 nm increases its intensity (Fig. ESI3-6†). This suggests that the binding of Cu^{II} at the ATCUN site, removes $V^{IV}O$ from this site, but increases its binding at another site, possibly the MBS. When >1 mol equivalent of Cu^{II} is added, additional and progressive changes are observed and at the end basically a pure HSA–Cu^{II} (1 : 2) is obtained – see Fig. 5. The EPR spectra depicted in Fig. 6 show a similar trend: up to the addition of 0.6 mol equivalents of Cu^{II} the spectra appear to be due to $V^{IV}O$; after addition of 0.8 mol equivalents the spectra clearly become a mixture of the signals of both metal ions. In the spectrum measured with a molar ratio of 1 : 5 : 1.3 (HSA : $V^{IV}O$: Cu^{II}) the $V^{IV}O$ resonances are not visually detected but the simulation confirmed its presence. Above this value the copper signal increases in intensity and two Cu^{II} resonances are observed after the ratio 1 : 5 : 1.6, which correspond to copper coordinated at the ATCUN and MBS sites. The $V^{IV}O$ displaced by Cu^{II} binding to the bulk solution yields species such as $[(V^{IV}O)_2(OH)_5]^-$,[46,47] and V^{IV} might also oxidize to V^{V}. These experiments lead us to state that the $V^{IV}O$–HSA system is very difficult to reproduce and the two experiments with Cu^{II} show that there is no thermodynamic equilibrium, the spectra recorded showing some dependence on the order of addition of the components. Our conclusion is that two types of independent $V^{IV}O$ sites must be assumed to describe the $V^{IV}O$–HSA system: the first type (only one site) is able to bind two $V^{IV}O$ centres as a dinuclear unit – EPR silent (almost) and CD active, assigned to the MBS, while each of the other type (one or more sites) is able to bind one $V^{IV}O$ as a monomer – EPR active and low CD activity. However, none of these sites is fully saturated with $V^{IV}O$ at *e.g.* 5 : 1 ratio (HSA : $V^{IV}O$) and this is why we see increasing spectroscopic signals with increasing amounts of $V^{IV}O^{2+}$ ions added, without reaching saturation.

$V^{IV}O$–HSA stability constants

Garribba *et al.* determined the stability constants of $(V^{IV}O)_2HSA$ and $(V^{IV}O)HSA$ complexes (Table 2) *via* frozen solution EPR measurements.[14] Their model allows an adequate interpretation of a significant part of the experimental data. When this model was applied to fit our room temperature EPR spectral data (ESI4 and 5†), it became clear that the model can be used only with the assumption of two independent $V^{IV}O$-sites: one which is able to bind two $V^{IV}O$ centres as dinuclear units, while the other type of binding is able to bind (at least partly) one $V^{IV}O$ as a monomer.

The experiments and the model reported here allowed us to determine the stability constants with smaller uncertainty than Garribba *et al.* (Table 2). However, the two data sets are in very good agreement with each other, only the stability constants of the $(V^{IV}O)_2HSA$ are somewhat smaller than those derived from frozen solution EPR measurements. The speciation of the $V^{IV}O$–HSA system is depicted in Fig. 7; as expected, the relative amount of dinuclear species increases with $c(V^{IV}O)$. This diagram also clearly shows that, in the therapeutically important

Table 3 Spin Hamiltonian parameters of the ternary complexes formed in the $V^{IV}O$–carrier ligand–HSA and $V^{IV}O$–carrier ligand–model ligand systems

		EPR					
Ligand	Complex	$g_\perp$	$A_\perp$[a]($\times 10^4$ cm^{-1})	$g_\parallel$	$A_{\parallel\perp}$ ($\times 10^4$ cm^{-1})	T (K)	Ref.
dhp	$V^{IV}OL_2$(HSA)			1.947	162.1	123	30
dhp	$V^{IV}OL_2$(MeIm)[a]			1.947	163.0	123	30
mal	$V^{IV}OL_2$(HSA)[a]	1.98/1.977	59.0/54.0	1.946	163.2	130	1
mal	$V^{IV}OL_2$(HSA)[a]	1.973(1)	58.0(0)	1.943(1)	161.1(4)	RT	
mal	$V^{IV}OL_2$(HSA)	1.976	56.9	1.943	166.1	77	
mal	$V^{IV}OL_2$(MeIm)[a]	1.980/1.977	60.0/55.0	1.944	164.8	130	1
mal	$V^{IV}OL_2$(HisOH)	1.973	56.8	1.940	165.5	77	
mal	$V^{IV}OL_2$(GlyHis)	1.973	56.8	1.941	165.5	77	
hpno	$V^{IV}OL_2$(HSA)	1.974(1)	57.2(4)	1.944(1)	159.4(4)	RT	
pic	$V^{IV}OL_2$(HSA)			1.950	159.7	123	30
pic	$V^{IV}OL_2$(HSA)	1.976(1)	57(1)	1.946(1)	158(1)	RT	
pic	$V^{IV}OL$(HSA)	1.975(1)	58(1)	1.943(1)	163(1)	RT	
pic	$V^{IV}OL_2$(MeIm)			1.943	158.8	123	30

[a] Rhombic spectra: g_x/g_y or A_x/A_y.

concentration range, the $(V^{IV}O)_2$HSA is in equilibrium with the monomeric $(V^{IV}O)$HSA species. Additionally, under conditions of metal ion excess the hydrolysis of $V^{IV}O$ does not allow the monomeric $(V^{IV}O)$HSA complex to reach its theoretical maximum.

$V^{IV}O$–HSA ternary complexes

One important aspect that should be addressed is how ligands, which are drug candidates for the treatment of diabetes, interact with $V^{IV}O$ in blood. In fact, even if the complex decomposes at the site of absorption, there is still the possibility of interaction between the ligand and $V^{IV}O$ in circulation. Maltol is one of the ligands used to complex $V^{IV}O$ that has been found to be more efficient *in vivo* than $V^{IV}O$ salts, probably due to enhanced absorption.[1,48] Other insulin mimetic complexes include the ligands pic, hpno and dhp.[49] The formation of hydrolytic species of VO(IV) and the ternary hydroxo complexes ($V^{IV}OA_2OH$, $(V^{IV}OAOH)_2$ in the case of pic and mal) were taken into account in the data fitting and the calculation of the stability constants. Oxidation of VO(IV) was not observed under our experimental conditions.

Several titrations of solutions containing HSA–$V^{IV}O$ and maltol were followed by CD in the visible range and by EPR; ESI4† shows examples of these. Fig. ESI4-2† shows that upon addition of the ligand the CD spectra completely change their pattern and increase in intensity. The X-band EPR spectra measured at 77 K (Fig. ESI4-1†) show that the amount of paramagnetic species increases upon addition of the ligand. The spin Hamiltonian parameters are included in Table 3 and the formed species are assigned to the ternary complex $V^{IV}OL_2$(HSA). Modeling studies with amino acids and peptides help to predict the possible donor groups on HSA that may coordinate to $V^{IV}O$.

Among all of the bio-ligands tested, the only system which retrieved similar vis CD spectra were obtained by titrating $V^{IV}O(mal)_2$ with Gly-L-His (see *e.g.* spectra included in Fig. ESI4-2†). The EPR spectra obtained at 77 K for this system show a major species with EPR parameters similar to those obtained in HSA–$V^{IV}O$–maltol: $A_\parallel = 166.2 \times 10^{-4}$ cm^{-1} and $g_\parallel = 1.944$. When similar studies were carried out with L-histidinol (L-HisOH) similar EPR parameters were also obtained (Table 3) and the CD spectra appear to be similar, but their intensity is very low. Comparison of the structures of Gly-L-His and L-HisOH, leads us to assume that the coordination of the imidazole nitrogen donors are responsible for the observed CD spectra and EPR parameters in these model systems. These results indicate that the imidazole nitrogen is relevant in the binding of $V^{IV}O$ to HSA and in the formation of the ternary species. Similar conclusions have been reported by Garribba *et al.*[14]

Several CD and EPR spectra were measured with solutions containing $V^{IV}O(maltolato)_2$ and adding chiral bio-ligands, *e.g.* L-His, L-Asp, L-Cys, Gly-L-Asp, Gly-L-His, L-histidinol.

The RT EPR measurements with dhp, mal, hpno and pic further confirmed these findings. On addition of different amounts of ligand to a 1 : 1 $V^{IV}O$: HSA system, the RT EPR spectra of these samples can be deconvoluted into an isotropic (with intensity I_I) and an anisotropic (with intensity I_A) spectra (Fig. 8A). For each system the isotropic part is the same as in the absence of HSA, and identical to the spectrum of the corresponding $V^{IV}OL_2$ complexes. The anisotropic part of the spectra can be assigned to ternary $V^{IV}O$–HSA–L species. Simulation of the measured spectra and double integration of the deconvoluted isotropic and anisotropic parts allowed the determination of the molar ratio between the ternary $V^{IV}O$–HSA–L species formed and the $V^{IV}OL_2$ complexes. These ratios were independent of the ligand excess in the cases of dhp (if $c_{dhp} > 1$ mM), hpno and mal (Fig. 9), indicating the formation of only a $V^{IV}OL_2$(HSA) species, in agreement with the earlier findings based on frozen solution EPR measurements.[12] However, HSA binds the various $V^{IV}OL_2$ complexes with different strengths, following the stability sequence: hpno > pic ≥ mal > dhp.

Titration of HSA with $V^{IV}O(mal)_2$, followed by RT EPR measurements, was carried out up to an HSA : $V^{IV}O(mal)_2$ ratio

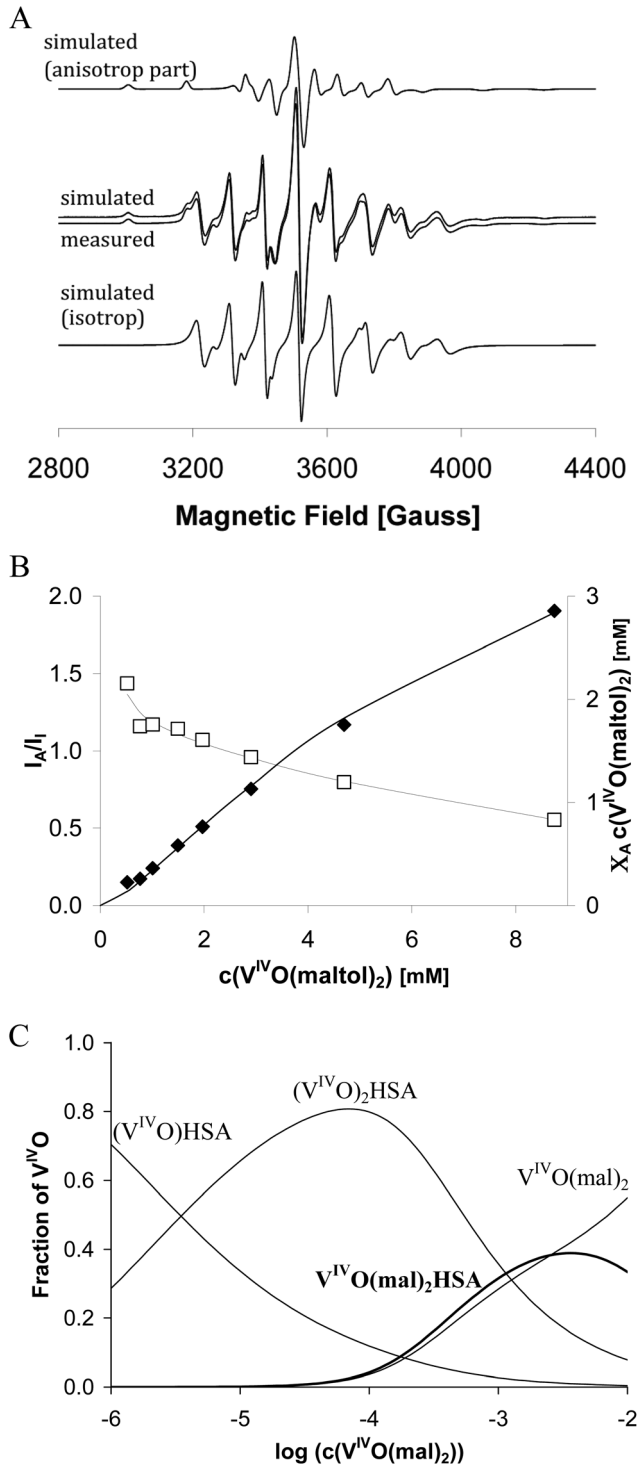

Fig. 8 (A) Simulation and "deconvolution" of a selected RT EPR spectrum measured at HSA : $V^{IV}O(mal)_2$ ratio of 1 : 7.8 (pH 7.4). (B) Left *y* axis: I_A/I_I (calculated ratio between the double integrated anisotropic and isotropic part of the simulated spectra) plotted as □; right *y* axis: the total concentration (in mM) of $V^{IV}O(mal)_2$ bound to HSA ($I_A/(I_I + I_A)c(V^{IV}O)$) plotted as ◆; HSA: 1.0 mM, as the concentration of $V^{IV}O(mal)_2$ is varied at (pH 7.4). The fitting shows the $n = 7$ case. (C) Calculated speciation of $V^{IV}O$. HSA: 1.0 mM, pH = 7.4, concentration of $V^{IV}O(mal)_2$ varied.

of 1 : 8. Saturation was not observed, and at 8-fold excess one HSA was able to bind 2.8 equivalents of $V^{IV}O(mal)_2$ (Fig. 8B).

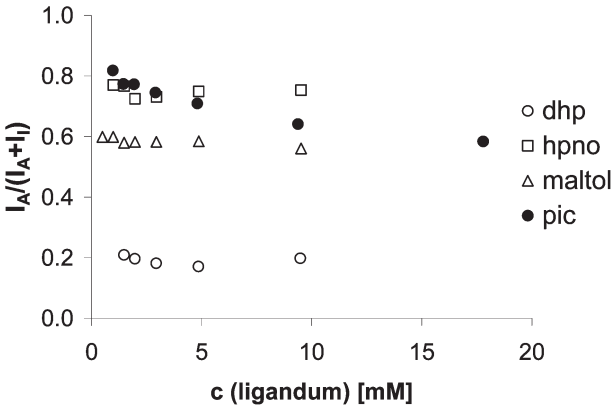

Fig. 9 The molar fraction of the ternary $V^{IV}OL_2$–HSA complexes calculated from the double integration of the deconvoluted isotropic and anisotropic parts of the spectra ($I_A/(I_A + I_I)$). HSA/$V^{IV}O$ 1 mM/0.5 mM, ligand concentration varied (pH 7.4).

Table 4 The conditional formation constants of the ternary $V^{IV}OL_x$(HSA) and $V^{IV}OL_x$(MeIm) complexes with various drug candidate ligands

	Log K^a				Log K^c		
Lig.	$n = 1^d$	$n = 7^d$	$n = 10^d$	Log K^b	$n = 1^d$	$n = 7^d$	$n = 10^d$
dhp	2.55(13) 3.1[f]	1.70[e]	1.55[e]	2.39[e]	—	—	—
mal	3.05[e]	2.22(2)	1.99(3)	4.5[g]	—	—	—
hpno	3.76(14)	2.91[e]	2.76[e]	—	—	—	—
pic	3.2[e]	2.4(3)	2.2(3)	2.67[e]	0.4[e]	−0.5(6)	−0.6(5)

[a] *K*: $V^{IV}OL_2$ + HSA = $V^{IV}OL_2$(HSA). [b] *K*: $V^{IV}OL_2$ + MeIm = $V^{IV}OL_2$(MeIm). [c] *K*: $V^{IV}OL_2$ + HSA = $V^{IV}OL$(HSA) + L. [d] For the explanation of *n*, see text. [e] Calculated based on log *K* (*n* = 1) = log *K* (*n* = 7) + log 7 = log *K* (*n* = 10) + log 10. [f] Calculated from ref. 16. [g] Taken from ref. 1.

This means that HSA has several sites where $V^{IV}O(mal)_2$ binds. Fitting (ESI5-3†) of the experimental data (concentration of bound and free $V^{IV}O(mal)_2$ determined by the double integration of the EPR spectra) allowed to estimate the number of binding sites (*n*). Assuming these binding sites are equivalent, $n = 7$ gave the best result (ESI5-3C†), however due to the small differences in fitting $n = 6$ or 8 cannot be excluded. As the non-equivalence of the sites is also a possibility, we can state that $n \geq 6$, but from our measurements it is not possible to determine the exact number, which may be as high as $n \sim 10$.

During the titrations not all $V^{IV}O$ centres were detectable by EPR, suggesting that a fourth, EPR silent species, $(V^{IV}O)_2HSA$ may also be involved in the equilibrium. This titration allowed the calculation of the stability constants of $(V^{IV}O)_2HSA$.

The logarithms of the stepwise stability constants in the cases of $n = 1$, 7 and 10 for the four different ligands are given in Table 4. Stepwise stability constant were determined also for 1-MeIm, and proved similar for HSA. The interaction between $V^{IV}O(dhp)_2$ and HSA was not as strong as predicted by other authors.[30]

The case of picolinic acid is different and our results are partly in disagreement with the earlier findings.[30] Among the EPR

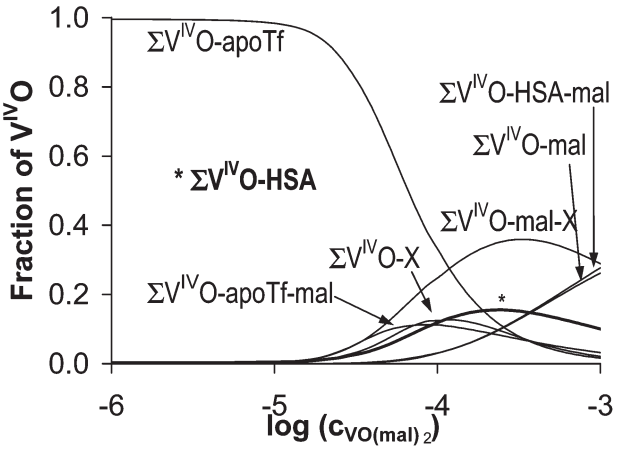

Fig. 10 Calculated speciation of $V^{IV}O(mal)_2$ in the blood serum: pH = 7.4, $c(HCO_3^-)$ = 25.0 mM, T = 25 °C. X could represent either phosphate or citrate. The concentration range relevant to oral administration of V is ≤10 μM. The concentrations: c(apoTf) = 37 μM, c(HSA) = 630 μM, $c(Fe^{III})$ = 25 μM, c(citrate) = 99 μM and c(phosphate) = 1.1 mM

active species (based on RT EPR), the molar fractions of the ternary complex $V^{IV}O$–HSA–L were dependent on the ligand excess. The amount of the "protein bound" $V^{IV}OL_2$ complex decreased with increasing total concentration of pic (Fig. 9), which indicates that not only $(V^{IV}OL_2)_n$(HSA) but also $(V^{IV}OL)_n$(HSA)-type species are formed. The difference in the spin Hamiltonian parameters for the last two species confirms their existence (Table 3).

The RT EPR titration of HSA with $V^{IV}O(pic)_2$ shows (similarly as for $V^{IV}O(mal)_2$) that there is more than one binding position. At an HSA : $V^{IV}O(pic)_2$ ratio of 1 : 5.5, 2.7 equivalents of $V^{IV}O$ exist either in the $V^{IV}OL$(HSA) or in the $V^{IV}OL_2$(HSA) form; the number of the binding sites (n), also in this case is most probably at least 6. The EPR spectral parameters of the ternary $V^{IV}O$–carrier ligand–HSA species formed are presented in Table 3. The most characteristic A values of $V^{IV}OL_2$(HSA) and $V^{IV}OL_2$(1-MeIm) are in good agreement, confirming the formation of the same or similar binding modes.

Conclusions

We show that human serum albumin is able to bind vanadium in at least two independent and different binding sites. By competition studies these are assigned to involve amino acid side chains of the ATCUN and MBS sites. The spectroscopic studies indicate that vanadium binds (at least partly) as a monomer at the ATCUN site and as an EPR silent dinuclear species at the MBS site.

The stability constants for $(V^{IV}O)$HSA and $(V^{IV}O)_2$HSA species were determined by RT EPR experiments and are in agreement with those obtained by frozen solution EPR measurements by Garribba *et al.*[14]

The studies carried out in the presence of carrier ligands confirms the formation of ternary systems and allowed the determination of the corresponding stability constants. Speciation diagrams show that for physiologically relevant $V^{IV}O$ concentrations (~1 μM, but definitely <10 μM), the most important species are $(V^{IV}O)$HSA and $(V^{IV}O)_2$HSA in the cases of maltol and picolinic acid.

In the serum at such concentration range (<10 μM) the much stronger binder apotransferrin or transferrin (apoTf or Tf) is the only relevant transporter (Fig. 10). HSA could become a $V^{IV}O$ binder only at higher metal ion concentration (≥20 μM, when Tf is getting saturated). Until the metal ion concentration does not reach 50 μM, HSA, if able to bound vanadium, replaces the original carrier ligands (mal, pic).

It means that if $V^{IV}O$ concentration is lower than 50 μM in serum, HSA does not help to prevent the decomposition of $V^{IV}O(mal)_2$. This is further evidence that vanadium is the active metabolite and the ligands, for example maltol, have only a carrier function.

It should, however, be mentioned that at higher than 50 μM $V^{IV}O$ concentration, which probably could be therapeutically relevant only for example in anticancer applications, the complex $V^{IV}O(mal)_2$ can partly survive the transport in serum and could reach the target cells.

Acknowledgements

The work was supported by the Hungarian National Research Fund (OTKA K77833), the Hungarian–Portuguese Bilateral Research Fund (TéT 09/2008). TJ thanks for the János Bolyai Research Scholarship of the Hungarian Academy of Sciences. JCP and IC thank FEDER, Fundação para a Ciência e Tecnologia, the Ciencia 2007 programme, the Portuguese NMR Network (IST-UTL Center) and PEst-OE/QUI/UI0100/2011.

References

1 G. R. Hanson, B. D. Liboiron, K. H. Thompson, E. Lam, N. Aebischer and C. Orvig, *J. Am. Chem. Soc.*, 2005, **127**, 5104–5115.
2 D. Rehder, *Bioinorganic Vanadium Chemistry*, John Wiley & Sons Ltd, England, 2008.
3 A. M. Evangelou, *Crit. Rev. Oncol. Hematol.*, 2002, **42**, 249–265.
4 O. J. D'Cruz and F. M. Uckun, *Expert Opin. Invest. Drugs*, 2002, **11**, 1829–1836.
5 J. C. Pessoa, A. Papaioannou, M. Manos, S. Karkabounas, R. Liasko, A. M. Evangelou, I. Correia, V. Kalfakakou and T. Kabanos, *J. Inorg. Biochem.*, 2004, **98**, 959–968.
6 D. Gambino, P. Noblia, M. Vieites, B. S. Parajon-Costa, E. J. Baran, H. Cerecetto, P. Draper, M. Gonzalez, O. E. Piro, E. E. Castellano, A. Azqueta, A. L. de Cerain and A. Monge-Vega, *J. Inorg. Biochem.*, 2005, **99**, 443–451.
7 D. Gambino, J. Benitez, L. Guggeri, I. Tomaz, J. C. Pessoa, V. Moreno, J. Lorenzo, F. X. Aviles and B. Garat, *J. Inorg. Biochem.*, 2009, **103**, 1386–1394.
8 M. R. Maurya, A. A. Khan, A. Azam, A. Kumar, S. Ranjan, N. Mondal and J. C. Pessoa, *Eur. J. Inorg. Chem.*, 2009, 5377–5390.
9 S. Shigeta, S. Mori, T. Yamase, N. Yamamoto and N. Yamamoto, *Biomed. Pharmacother.*, 2006, **60**, 211–219.
10 A. Maiti and S. Ghosh, *J. Inorg. Biochem.*, 1989, **36**, 131–139.
11 P. Ghosh, O. J. D'Cruz, D. D. DuMez, J. Peitersen and F. M. Uckun, *J. Inorg. Biochem.*, 1999, **75**, 135–143.
12 T. Kiss, T. Jakusch, D. Hollender, A. Dornyei, E. A. Enyedy, J. C. Pessoa, H. Sakurai and A. Sanz-Medel, *Coord. Chem. Rev.*, 2008, **252**, 1153–1162.
13 E. Kiss, K. Kawabe, A. Tamura, T. Jakusch, H. Sakurai and T. Kiss, *J. Inorg. Biochem.*, 2003, **95**, 69–76.
14 E. Garribba, D. Sanna and G. Micera, *J. Inorg. Biochem.*, 2009, **103**, 648–655.

15 A. Sanz-Medel, T. Jakusch, D. Hollender, E. A. Enyedy, C. S. Gonzalez, M. Montes-Bayon, J. C. Pessoa, I. Tomaz and T. Kiss, *Dalton Trans.*, 2009, 2428–2437.
16 E. Garribba, D. Sanna, P. Buglyo and G. Micera, *J. Biol. Inorg. Chem.*, 2010, **15**, 825–839.
17 J. C. Pessoa and I. Tomaz, *Curr. Med. Chem.*, 2010, **17**, 3701–3738.
18 W. R. Harris, S. B. Friedman and D. Silberman, *J. Inorg. Biochem.*, 1984, **20**, 157–169.
19 D. Sanna, G. Micera and E. Garribba, *Inorg. Chem.*, 2011, **50**, 3717–3728.
20 D. Sanna, L. Biro, P. Buglyo, G. Micera and E. Garribba, *Metallomics*, 2012, **4**, 33–36.
21 C. A. Blindauer, J. Lu, A. J. Stewart, P. J. Sadler and T. J. T. Pinheiro, *Biochem. Soc. Trans.*, 2008, **36**, 1317–1321.
22 T. Peters Jr, *All About Albumin: Biochemistry, Genetics, and Medical Applications*, Academic Press, San Diego, CA, 1996.
23 W. Bal, J. Christodoulou, P. J. Sadler and A. Tucker, *J. Inorg. Biochem.*, 1998, **70**, 33–39.
24 P. J. Sadler, A. J. Stewart, C. A. Blindauer, S. Berezenko and D. Sleep, *Proc. Natl. Acad. Sci. U. S. A.*, 2003, **100**, 3701–3706.
25 C. A. Blindauer, I. Harvey, K. E. Bunyan, A. J. Stewart, D. Sleep, D. J. Harrison, S. Berezenko and P. J. Sadler, *J. Biol. Chem.*, 2009, **284**, 23116–23124.
26 H. Sakurai, H. Yasui and Y. Kunori, *Chem. Lett.*, 2003, **32**, 1032–1033.
27 H. Sakurai, H. Yasui and K. Takechi, *J. Inorg. Biochem.*, 2000, **78**, 185–196.
28 N. D. Chasteen and J. Francavilla, *J. Phys. Chem.*, 1976, **80**, 867–871.
29 T. Kiss, T. Jakusch, J. C. Pessoa and I. Tomaz, *Coord. Chem. Rev.*, 2003, **237**, 123–133.
30 E. Garribba, D. Sanna and G. Micera, *Inorg. Chem.*, 2010, **49**, 174–187.
31 G. Micera, D. Sanna and E. Garribba, *Inorg. Chem.*, 2009, **48**, 5747–5757.
32 K. Hirayama, S. Akashi, M. Furuya and K. Fukuhara, *Biochem. Biophys. Res. Commun.*, 1990, **173**, 639–646.
33 L. Vellenga, T. Wensing, H. J. A. Egberts, J. E. Vandijk, J. M. V. M. Mouwen and H. J. Breukink, *Vet. Res. Commun.*, 1989, **13**, 467–474.
34 B. Yuan, K. Murayama and H. Yan, *Appl. Spectrosc.*, 2007, **61**, 921–927.
35 A. Rockenbauer and L. Korecz, *Appl. Magn. Reson.*, 1996, **10**, 29–43.
36 L. Z. I. Nagypál, *Computational Methods for the Determination of Stability Constants*, Plenum, New York, 1985.
37 G. P. L. Zékány and I. Nagypál, *PSEQUAD for Chemical Equilibria*, Technical Software Distributions, Baltimore, 1991.
38 T. Kiss, E. Kiss, G. Micera and D. Sanna, *Inorg. Chim. Acta*, 1998, **283**, 202–210.
39 P. Buglyo, T. Kiss, E. Kiss, D. Sanna, E. Garribba and G. Micera, *J. Chem. Soc., Dalton Trans.*, 2002, 2275–2282.
40 E. Kiss, E. Garribba, G. Micera, T. Kiss and H. Sakurai, *J. Inorg. Biochem.*, 2000, **78**, 97–108.
41 M. Valko, H. Morris, M. Mazur, J. Telser, E. J. L. McInnes and F. E. Mabbs, *J. Phys. Chem. B*, 1999, **103**, 5591–5597.
42 G. R. Willsky, A. B. Goldfine, P. J. Kostyniak, J. H. McNeill, L. Q. Yang, H. R. Khan and D. C. Crans, *J. Inorg. Biochem.*, 2001, **85**, 33–42.
43 I. Petitpas, T. Grune, A. A. Bhattacharya and S. Curry, *J. Mol. Biol.*, 2001, **314**, 955–960.
44 W. Bal, M. Rozga, M. Sokolowska and A. M. Protas, *J. Biol. Inorg. Chem.*, 2007, **12**, 913–918.
45 K. S. Iyer, S. J. Lau, S. H. Laurie and B. Sarkar, *Biochem. J.*, 1978, **169**, 61–69.
46 L. Vilas Boas and J. C. Pessoa, in *Comprehensive Coordination Chemistry*, ed. G. Wilkinson, R. D. Gillard and J. A. McCleverty, Oxford, 1987, vol. 3, pp. 453–583.
47 J. C. Pessoa, L. F. V. Boas, R. D. Gillard and R. J. Lancashire, *Polyhedron*, 1988, **7**, 1245–1262.
48 I. A. Setyawati, K. H. Thompson, V. G. Yuen, Y. Sun, M. Battell, D. M. Lyster, C. Vo, T. J. Ruth, S. Zeisler, J. H. McNeill and C. Orvig, *J. Appl. Physiol.*, 1998, **84**, 569–575.
49 M. Passadouro, A. M. Metelo, A. S. Melao, J. R. Pedro, H. Faneca, E. Carvalho and M. M. C. A. Castro, *J. Inorg. Biochem.*, 2010, **104**, 987–992.